BARRIER PROPERTY DETERMINATION AND LIFETIME PREDICTION BY ELECTROCHEMICAL IMPEDANCE SPECTROSCOPY OF A HIGH PERFORMANCE ORGANIC COATING

DETERMINACIÓN DE PROPIEDADES BARRERA Y DE PREDICCIÓN DE TIEMPO DE VIDA POR ESPECTROSCOPÍA DE IMPEDANCIA ELECTROQUÍMICA DE UN RECUBRIMIENTO ORGÁNICO DE ALTO RENDIMIENTO

JORGE ANDRÉS CALDERÓN-GUTIERREZ
DSc., Universidad de Antioquia - CIDEMAT, Medellín, Colombia. jacalder@udea.edu.co
FRANKY ESTEBAN BEDOYA-LORA
MEng., Universidad de Antioquia - CIDEMAT, Medellín, Colombia. frankybedoya@gmail.com

Received for review March 28 th, 2013, accepted September 20th, 2013, final version September, 24 th, 2013

ABSTRACT: The anticorrosion performance of an Epoxy-Mastic organic coating was evaluated during continuous immersion in saline solution using electrochemical impedance spectroscopy (EIS). The typical parameters of pore resistance and charge transfer resistance were determined employing an equivalent electric circuit. Constant phase elements (CPE) were used in order to determine fraction of water absorbed, mass diffusion, solubility and the swelling coefficients, as well as to predict the failure times of the coating. The results found by EIS measurements match very well with the high resistance to deterioration exhibited by the coating. It was also found that the excellent protection performance of the coating was mainly due to low water solubility and low permeability.

Key words: Organic coatings, electrochemical impedance spectroscopy, water diffusion, delaminated area, failure time prediction.

RESUMEN: El desempeño anticorrosivo de un recubrimiento orgánico tipo Epoxy-Mastic fue evaluado en condiciones de inmersión continua en solución salina usando espectroscopía de impedancia electroquímica (EIS). Se determinaron los parámetros típicos como la resistencia de poro y resistencia a la transferencia de carga usando un circuito eléctrico equivalente. Se usaron elementos de fase constante (CPE) para determinar la fracción de agua absorbida, coeficientes de difusión de masa, solubilidad y coeficientes de hinchamiento, así como también para predecir los tiempos de falla de dicho recubrimiento. Los resultados hallados por medio de medidas EIS concuerdan con la alta resistencia al deterioro que exhibe el recubrimiento. El excelente desempeño protector es debido principalmente a la baja solubilidad y permeabilidad de agua.

Palabras clave: Recubrimientos anticorrosivos, espectroscopía de impedancia electroquímica, difusión de agua, área delaminada, predicción de tiempos de falla.

1. INTRODUCTION

Two decades ago Haruyama [1] proposed a method for calculating the deterioration of organic coatings exposed to a corrosive environment using the equivalent circuit shown in Fig. 1. Haruyama's methodology phenomenologically explains the processes that occur inside organic coatings when they are exposed to an electrolyte and when there are minor defects or imperfections, such as small pores, in the coating. The Randles circuit (Fig. 2) has been used extensively to evaluate organic coatings that exhibit highly capacitive behavior or to evaluate pore-free coatings. However, the Randles circuit becomes useless after a few hours of continuous immersion because new time constants in the impedance spectra may appear. A complete description of each of the passive elements making up the two circuits shown in Fig. 1 and 2 can be found in numerous sources [2, 3]. The coating resistance (R_C) is closely related to the state of the coating, its additives or pigments, porosity and type of resin. The coating capacitance (C_C) is associated with the amount of water absorbed during the initial stages of exposure to the electrolyte [4]. The charge transfer resistance (R_{ct})

is directly related to the susceptibility to corrosion of the substrate and theoretically is the most appropriate parameter for measuring the protective properties of the coating [5]. The double layer capacitance (C_{dl}) is almost unanimously associated with the delaminated area of the coating [2]. When the diffusion process is shown in the impedance spectrum, the use of the Warburg impedance (Z_w) is normally accepted in order to give a physicochemical explanation to these processes [6].

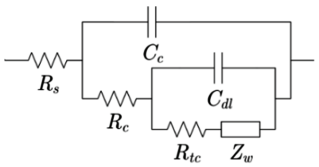

Figure 1. Equivalent electrical circuit used by Haruyama to explain the deterioration of a barrier organic coating using electrochemical impedance spectroscopy [1]

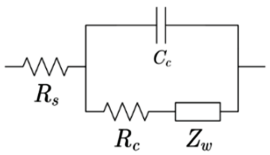

Figure 2. Randles circuit commonly used to simulate the electrochemical impedance of a defect-free barrier coating

2. THEORETICAL TREATMENT

The five EIS parameters described above have been used to evaluate the protective properties of organic coatings and even obtain empirical correlations [7-9]. However, when it is desired to adjust the EIS response using these passive elements of the equivalent circuit, in most cases, the fit is poor due to lack of uniformity in the coating or in the substrate [10]. Additionally, other phenomena can reduce the quality of the experimental EIS fit, for example geometrical effects such as polymer swelling [11], non-Fickian diffusion or variations in the time constants related to the corrosion processes. A commonly used alternative to reduce fit problems is to use constant phase elements (CPEs) instead of pure capacitances. It has been suggested that the existence of a distribution of relaxation times is the cause of CPEs [12]. A CPE can be thought of as an imperfect capacitor and allows a better fit of the experimental impedance when there is a flattening of the semicircle represented in the Nyquist plot [10, 13, 14]. According to Eq. 1, CPEs provides two terms: the pseudo-capacitance (Y_0) and an exponential constant (n).

$$Z = \frac{(j\omega)^{-n}}{Y_0} \tag{1}$$

In many cases the pseudo-capacitance can be represented as a simple capacitance (occurring when $n = 1$ since there is an absence of deviations from ideality in a perfect capacitor, *i.e.* there are no interferences caused by factors already cited). When equations and empirical relationships are used it is necessary to perform a conversion that enables the computation of the actual capacitance from a simulated CPE. This can be done with Eq. 2 [15].

$$C_c = Y_c (\omega_{\max})^{n-1} \tag{2}$$

Now, considering $\omega_{max} = 1/RC$, where ω_{max} is the frequency of the local maximum in imaginary region obtained from the Nyquist diagram, the actual capacitance can be calculated with Eq. 3.

$$C_c = \frac{(Y_c R)^{\frac{1}{n}}}{R} \tag{3}$$

Using the above relationships, several methods have been developed to evaluate the performance of organic coatings, as well as correlations and methods derived from the parameters obtained by the use of the circuit proposed by Haruyama (Fig. 1). One of the most popular methods for evaluating the performance of organic coatings, but also subject to substantial restrictions, is the breakpoint frequency method. This method, initially proposed by Haruyama [1], describes the relationship between the delaminated area and the total area of the sample, in accordance with Eq. 4 and 5.

$$f_b = f_b^0 \frac{A_d}{A} \tag{4}$$

$$f_b^0 = \frac{1}{2\pi\rho\epsilon\epsilon_0} \tag{5}$$

Where A_d and A are the delaminated area and the total area of the substrate, respectively. f_b^0 is the proportion constant, which can be obtained from Eq. 5. ρ is the electrical resistivity of the coating. ϵ is the relative electric permittivity and ϵ_0 is the vacuum electric permittivity (8.86×10^{-14} *F/cm*). The breakpoint frequency can be obtained by performing a scan at high frequencies and is located exactly at the point where the phase angle falls for the first time to 45° [1].

One of the first approaches when studying the lifetime of an organic coating using electrochemical impedance measurements is to determine the time to failure of the coating. This is the time after which the coating no longer offers significant protection against corrosion. Eq. 6, obtained by Bierwagen [16], makes it possible to establish the time after which a coating fails, according to an arbitrary failure impedance value.

$$t_{fail} = \theta \left[\ln \left(\frac{|Z|_0 - |Z|_m}{|Z|_{fail} - |Z|_m} \right) \right] \quad (6)$$

Where $|Z|_m$ is the impedance modulus of the substrate, $|Z|_0$ is the initial coating module and θ is considered as the characteristic decay time of the material. The difficulty of this method is in establishing a real value for $|Z|_{fail}$ from which it can be assumed that the coating has lost its protective properties. The impedance module used in this equation must be taken at a low experimental impedance frequency range, generally between 1×10^{-3} and 5×10^{-3} [16]. A coating is usually considered to have inadequate protection when the charge transfer resistance exhibits values below 10^6 ohm [10].

All organic coatings are somewhat permeable. This permeability may worsen with the addition of certain types of pigments, for example zinc powders, producing a significant reduction in the barrier property. However, there is an increase in the corrosion resistance of the coatings after prolonged periods when coating has a pigment volume concentration (PVC) greater than 60 [17]. The absorbed water content is of special interest since once the polymer has been saturated with water, even in the absence of electro-active species, the occurrence of corrosion phenomena, swelling, loss of adhesion and deterioration of mechanical properties of the coating are significantly enhanced. Furthermore, it has been found that the diffusion of water controls the start time of delamination and consequently the loss of protective capacity [18, 19].

The parameter most related to the amount of water absorbed is the coating capacitance, (C_C), expressed as:

$$C_c = \epsilon \epsilon_0 \frac{A}{d} \quad (7)$$

Coating capacitance is directly related to the electrical permittivity of the medium (ϵ), the permittivity of the vacuum (ϵ_0), the coating area (A), and the thickness of the coating (d). When the absorption process starts, coating capacitance changes due to the incorporation of water molecules. Water has a relative permittivity of 80, while the resins used in anticorrosive coatings have permittivity value typically in the range of 2.5 to 10. Therefore, the more water absorbed, the greater the capacitance.

Brasher and Kinsgbury [20], in their widely cited research, proposed a relationship to calculate the amount of water absorbed. This relationship is shown by Eq. 8.

$$X_v = \frac{\log\left(C_{c(t)} / C_{c(0)}\right)}{\log 80} \quad (8)$$

Where X_v is the fraction volume of absorbed water, and $C_{c(t)}$ and $C_{c(0)}$ are the capacitance of the coating at a given time and at the initial time, respectively. To make use of this expression it is necessary to fulfill several requirements, such as the absence of swelling in the coating, homogeneous distribution of the water, and absence of polar solvents. Additionally, the fraction of water absorbed must be relatively small [21]. Furthermore, it has been numerically shown that the values reported with this equation differ considerably from gravimetric data [22]. If the above conditions are satisfied, mathematical expressions may be obtained for calculating the diffusivity of the water using the relationship proposed by Brasher-Kingsbury. Eq. 9 for example, can be used to calculate water diffusivity [18], whereas more complex correlations can be used to obtain the swelling coefficients, such as Eq. 10 [11, 23].

$$\frac{\ln C_{c(t)} - \ln C_{c(0)}}{\ln C_{c(\infty)} - \ln C_{c(0)}} = \frac{2\sqrt{D}}{L\sqrt{\pi}}\sqrt{t} \quad (9)$$

$$\log C_t = \log\left(\frac{C_{c(\infty)}}{C_{c(0)}}\right) \left\{1 - \frac{8}{\pi^2}\sum_{n=0}^{\infty}\frac{1}{(2n+1)^2}\exp\left[\frac{-(2n+1)^2 D\pi^2}{4L^2}t\right]\right\} + SC_c t + \log C_0 \quad (10)$$

As previously mentioned, $C_{c(0)}$ and $C_{c(t)}$ are the initial coating capacitance and the coating capacitance at a given time, respectively. $C_{c(\infty)}$ is the capacitance of water saturated coating, *i.e.* when the capacitance does not vary significantly with time. D is the diffusion coefficient of water in the coating. L and SC_c are the thickness and swelling coefficient of the coating respectively.

The solubility (S) and the permeation coefficient (P) can be calculated with simple relationships expressed in Eq. 11 and 12 respectively. These parameters are usually employed for comparison purposes.

$$S = \frac{V_\infty}{V_c + V_\infty} \times \rho_w = \frac{\log C_{c(\infty)} / C_{c(0)}}{\log 80} \times \rho_w \quad (11)$$

$$P = D \times S \quad (12)$$

Where ρ_w is the water density in $kg.m^{-3}$ and V_∞ and V_c are the volume occupied by the water to infinite time and the volume of the dry coating respectively.

2. MATERIAL AND METHODS

Carbon steel specimens were prepared by sandblasting to white metal grade SP-3, followed by washing with a mixture of ethanol/water and degreasing with acetone before applying the organic coating. The steel samples were painted with a commercial high solids epoxy mastic coating by spraying. In order to facilitate the coating application, 30% v/v of solvent was added. Table 1 shows general characteristics of the coating. Additionally, the coating was characterized by Micro-Raman Spectroscopy (Micro-Raman, HoribaJovinYvon), in order to corroborate the coating composition. As can be seen in Raman spectrum shown in Fig. 3, the characteristic vibration bands related with polydiphenylsiloxane [24], titanium dioxide (rutile phase) as pigment [25] and epoxy compounds [26] appear in the Raman spectrum. This is in agreement with information presented in Table 1.

Table 1. General characteristics of the studied coating

Coating	Epoxi Mastic Polysiloxane
Chemical nature	Epoxy-silicone hybrid
Catalyzer	Organosilane
Pigments	TiO_2, $CaSiO_3$, Silica
Solid Volume	93 % (Catalyzed)

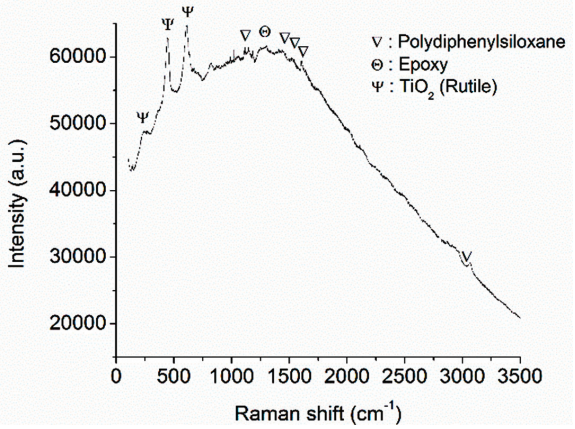

Figure 3. Raman spectra of mastic epoxy coating

Before the test, the painted specimens were kept in a natural dry room for 4 weeks to achieve a convenient curing and drying of the coating. The average thickness of the coatings dry film was 172 ± 19 microns. The painted steel coupons were exposed in continuous immersion in a 3% NaCl solution (0.5M NaCl) for about 440 days. The protective properties of the coating and corrosion phenomena were evaluated by measuring open-circuit potential and electrochemical impedance over time, following visual inspection. Electrochemical tests were conducted with a conventional three electrode cell, using the painted samples (38.5 cm^2 exposed area) as the working electrode. A saturated calomel electrode (SCE) and Pt plate were used as reference and counter electrodes respectively. The impedance measurements were performed at open circuit potential in a frequency range of 40 kHz to 3 mHz, using a perturbation amplitude of 10 mV. An AUTOLAB PGSTAT-30 potentiostat/galvanostat was used.

3. RESULTS AND DISCUSSION

Fig. 4 shows the Nyquist and Bode plots of impedance measurements of epoxy mastic coating taken during 441 days of continuous immersion in 0.5 M NaCl solution. The excellent performance and the efficient barrier protection at the beginning of the test can be clearly seen, as practically all diagrams consist of an open capacitive loop, with impedance values of 10^{10} ohm.cm^2. The capacitive loop tends to lean toward the real axis as the time of immersion increases, which means diminishing of the coating resistance and increases of capacitance due to electrolyte permeation.

Fig. 5 presents the evolution of the resistances related to the coating/metal system. The coating resistance (R_C) and charge transfer resistance (R_{ct}) tend to fall during the first days of immersion as a result of the absorption of water and the establishment of oxy-reduction reactions at the metal-electrolyte interface. However, this process seems to stop after 100 days of immersion since the charge transfer resistance tends to stabilize after this time. The modulus of the impedance follows the behavior of the charge transfer resistance more closely than the resistance of the coating. This suggests that the evaluation of the general anticorrosive performance of the coating should be done preferably by assessing the behavior of the (R_{ct}) during the evaluation time. It can be seen (R_{ct}) does not fall below a protection level value of 10^6 ohm.cm$^{2.}$ at any time and that (R_C) is also maintained high, although with a tendency to decrease. It was confirmed visually that there were no defects such as blistering, delamination, cracking or corrosion.

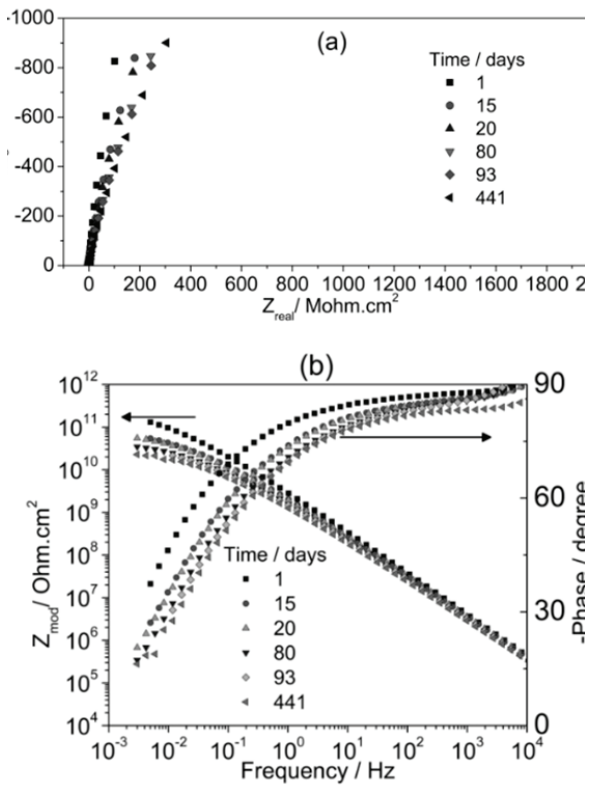

Figure 4. Electrochemical impedance spectra of epoxy mastic coating at different times of exposition in 3% NaCl solution: (A) Nyquist plots. (B) Bode plots

The open circuit potential (OCP) vs SCE values are presented in Fig. 6. A rapid evolution of (OCP) to anodic values was observed, from -250 mV in the first days of immersion up to -0.02 mV after 100 days, from then on the potential remained almost constant at -0.02 mV. The progressive increase of the OCP and stabilization in anodic values is consistent with that observed in the evolution of the (R_{ct}), which tends to remain constant after 100 days of exposure. The progressive increase of the OCP and its subsequent stabilization at positive potentials indicates the existence of an anodic control of the oxidation-reduction process on the metal substrate and the anodic area decreases as a result of the barrier imposed by the polymeric coating. Because of the high barrier property of the coating against the diffusion of oxygen molecules and the passage of the electrolyte, a cathodic control, which is commonly observed in the initial stages of the under-film corrosion process [27], is not present.

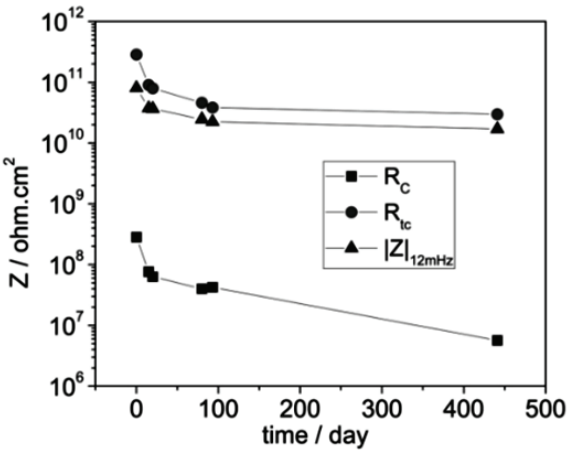

Figure 5. Evolution of coating resistance (R_C), charge transfer resistance (R_{tc}) and impedance module at 12 mHz ($|Z|_{12mHz}$) of epoxy mastic coating at different times of exposition in 3% NaCl solution

3.1. Delaminated Area

One of the most cited methods for delaminated area calculation is the breakpoint frequency method [1]. As mentioned in the introduction section of this work, to properly use this method the experimental measurements must match the impedance of the circuit of Fig. 1. Furthermore, the two time constants associated with the coating and the metal-coating interface must appear sufficiently spaced to allow the direct reading of the breakpoint frequency from the phase diagram. In this study, even though the experimental data fits

very well with the impedance of the electrical circuit using constant phase elements, the separation between the two time constants of the phenomena is not clear and the breakpoint frequency is not easily detected. For this reason the aforementioned analysis method is not suitable for the quantitative evaluation of the coating deterioration and coating delamination.

The inability to evaluate the anticorrosion performance of intact coatings by the breakpoint frequency method has previously been reported by Pistorius [28]. Pistorius establishes that intact coatings only show one time constant in the impedance spectrum or two time constants very close to each other. According to the Haruyama postulation, for a clear observation of the two time constants, the relationship $C_C.R_C << C_{dl}.R_{tc}$ must be satisfied. This situation prevents the accurate determination of the breakpoint frequency value.

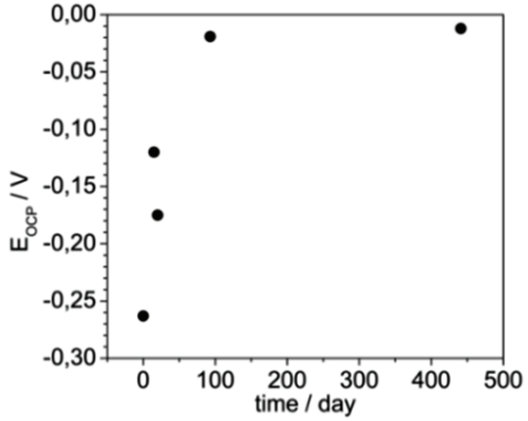

Figure 6. Open circuit potential vs SCE of epoxy mastic coating at different times of exposition in 3% NaCl solution

3.2. Failure time determination

The time to failure of the coating (t_{fail}) was calculated once parameter θ was known. The θ parameter can be easily obtained from Eq. 6 and by performing a linear regression of the impedance module (when $f \rightarrow 0$) versus immersion time. It was necessary to use a minimum frequency of 12 mHz to calculate the impedance module, since this is the lowest frequency that can be attained without data dispersion. The $|Z|_m$ value must be negligible compared to $|Z|_{fail}$. After completing the regression process, a slope of $1/\theta$ = 0.01058 was obtained, which corresponds to θ = 94.5 days. Upon defining a failure impedance of 9.9×10^6 *ohm.cm*^{2}, *i.e.* when the resistance of the system drops to the range of minimum protection (10^6 *ohm.cm*^{2}) [10, 29], the failure time found was t_{fail} = 851 days. This result is the predicted time from which the coating would not be expected to offer enough corrosion protection to the substrate under immersion conditions in 0.5 M NaCl solution, and coating damage signs would be observable. The experiment performed in this study was carried out for about 441 days. Neither coating damage nor signs of corrosion were observed during this time, as predicted by the Bierwagen expression [16] and experimentally corroborated using electrochemical impedances and visual inspection.

3.3. Fraction of water absorbed and diffusion coefficients for the Fick process

The calculation of the fraction of water absorbed X_v was performed using the Brasher and Kinsgbury expression [20], as can be seen in Eq. 8. The real coating capacitance (C_C) was calculated from the pseudo-capacitance (Y_C) and CPE values using Eq. 3. Fig. 7 shows the variation in the fraction of absorbed water (X_v) and the pseudo-capacitance (Y_C) during the immersion of metal coated samples in 0.5M NaCl solution. It can be seen that even after 441 days of immersion, no stabilization of the fraction of water absorbed is reached. Therefore, it can be said that complete water saturation of the epoxy mastic coating is not achieved. This corroborates the good performance of the barrier and anticorrosion properties of the coating, as the barrier properties are shown to persist longer than 400 days of immersion. The variation of the CPE exponential term for coating capacitance (n_c) over time is shown in Fig. 8. It can be seen that the value of n_c remains relatively constant during the first 120 days of immersion, indicating that there is little geometric variation of the polymer during immersion. This is due to the occurrence of low water absorption into the polymer during this period of time. After 120 days of immersion, a slight decrease of the n_c value can be observed, reaching a final value of 0.94 at the end of the immersion (441 days). This means that geometrical change, due to swelling of the polymer caused by water absorption, is only observable at longer immersion times. The swelling of the coating caused by water absorption could imply significant changes in the model of electrolyte diffusion through the polymer. Therefore, this must be taken into account

for the calculation of the diffusion coefficient for longer immersion times, as discussed in the next section.

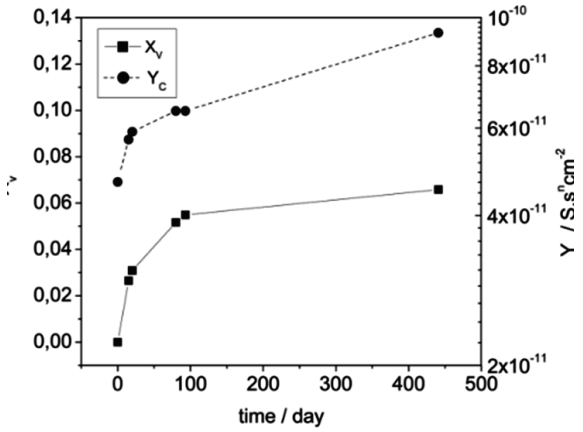

Figure 7. Coating pseudo-capacitance (Y_C), and water fraction (X_v) of epoxy mastic coating at different times of exposition in 3% NaCl solution

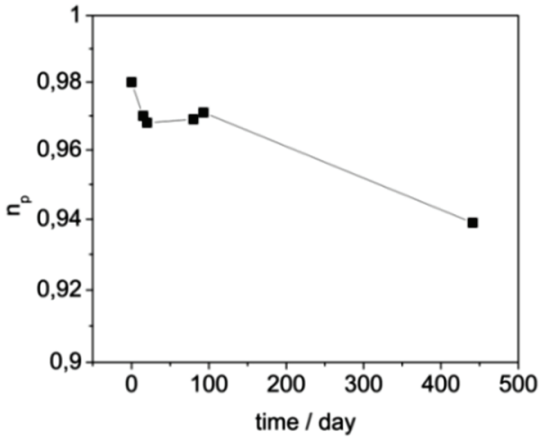

Figure 8. Exponential term n_c associated with the coating CPE at different times of exposition in 3% NaCl solution

The diffusion coefficient of water was calculated using Eq. 9. By plotting the left side of Eq. 9 vs the square root of the immersion time a linear behavior can be seen during the first 100 days of immersion, see Fig. 9. This behavior corresponds to a Fick type diffusion of the water through the coating. The calculated diffusivity value was $D_{AB} = 1.91\times10^{-15}\ m^2/s$. This diffusivity value is significantly lower compared to values reported for a conventional epoxy coating, which are in the range of $10^{-13}\ m^2/s$ [11, 18, 30, 31]. However, the low diffusivity value obtained for the epoxy mastic coating during the early stage of immersion is in agreement with the excellent anticorrosion performance showed by the coating, even after 400 days of continuous immersion. In order to verify the complete water diffusivity property of the epoxy mastic coating, a second calculation considering the film swelling due to water absorption was carried out. This calculation considered the nonlinear diffusion mechanism (non-Fickian diffusion process) shown by the coating during a longer immersion time. In addition, swelling and permeation coefficients of the coating can also be obtained.

3.4. Water diffusion coefficient for nonlinear behavior

The calculation of the non-Fickian diffusion and the swelling coefficients during water permeation into the coating was performed using Eq. 10. It was executed through a non-linear regression using the Levenberg-Marquardt algorithm and truncation at the 8th term when the summation counter was $n = 7$. It was also observed that truncation at lower terms leads to similar results. The swelling coefficient is an indirect measure of the interaction between the incoming electrolyte and the polymer. The swelling coefficient of the polymeric coating can be related to the variations of impedance parameters such as capacitance and the exponent (n_p) during the time of exposure to a corrosive media. The diffusion coefficient obtained by non-Fickian diffusion behavior was $D_{AB} = 2.55\times10^{-15}\ m^2/s$ and the swelling coefficient was $SC_C = 3.22\times10^{-12}\ s^{-1}$. It is important to highlight that the diffusion coefficients obtained by both linear and nonlinear methods give similar results. The low diffusivity and swelling coefficients obtained during the longer immersion period of the epoxy mastic coating is consistent with the excellent anticorrosion performance of the coating.

Using Eq. 11 and 12 it was possible to calculate the water solubility (S) and the permeation (P) coefficients of the epoxy mastic coating. The respective values were $S = 65.6\ kg.m^{-3}$ and $P = 1.67\times10^{-10}\ g.m^{-1}.s^{-1}$. The permeation coefficient is relatively low compared to that observed for other polymer materials, which exhibit P values in the range of $10^{-8}\ g.m^{-1}.s^{-1}$. Similarly, the water solubility coefficient of the epoxy mastic coating is also low compared to other polymers [32]. This may be the main reason why the coating has high barrier properties and high anticorrosion performance.

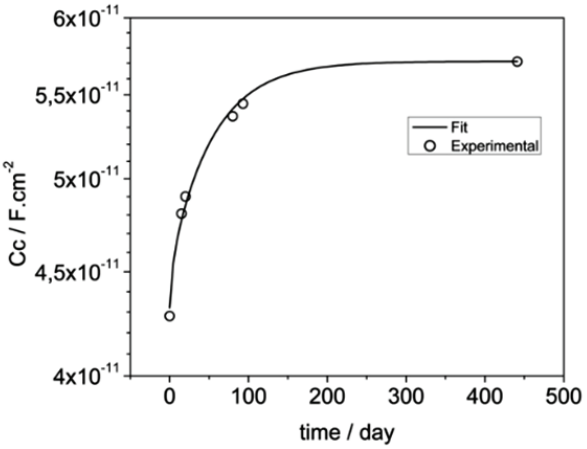

Figure. 9 Coating capacitance and fitting (Eq. 9)

3.5. Evaluation of an intentionally caused defect on delamination

During immersion of the epoxy mastic coating in 0.5M NaCl solution for 441 days, no visual signs of coating defects or corrosion phenomena were observed. However, due to the longer immersion time, some micro failures or micro blisters could have occurred, which if present would indicate the first stage of delamination. In order to verify if the electrochemical information of the metal/coating interface obtained from EIS measurements was correctly related with the anticorrosion coating performance, a small incision on the coating (0.2 mm x 5 mm) was made, as shown in Fig. 10. EIS measurements on coated samples with incisions were carried out during 14 h of immersion in 0.5M NaCl solution.

Fig. 10 shows photographs of coated samples with incision. As can be seen, no coating adhesion loss or increase in delamination area in the incision was observed. Fig. 11 shows Bode impedance diagrams of the coated samples with and without incisions at different immersion times. Unlike what was observed for samples without defects, which exhibited only one time constant, the impedance of the samples with incision exhibited two distinguishable time constants. The time constant at high frequencies can be related to the metal/electrolyte interface. The impedance modulus of this time constant is close to 10 kOhm.cm^2. This value is what is normally found for the charge transfer resistance of the metal/electrolyte interface in corrosion processes.

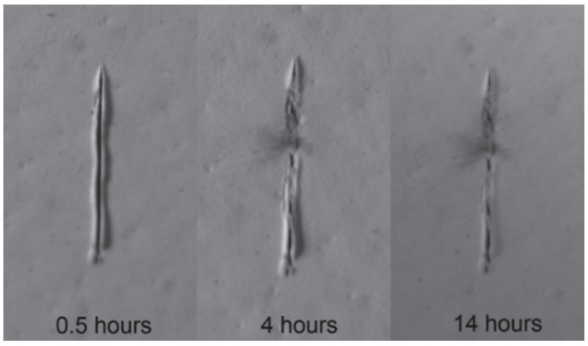

Figure 10. Coating photographs with incision at different times of immersion

The impedance modulus of the second time constant observed at a low frequency exhibits values close to 5 MOhm.cm^2. Clearly, these impedance modulus values cannot be related only with the coating but rather with metal corrosion processes under the coating near to the incision.

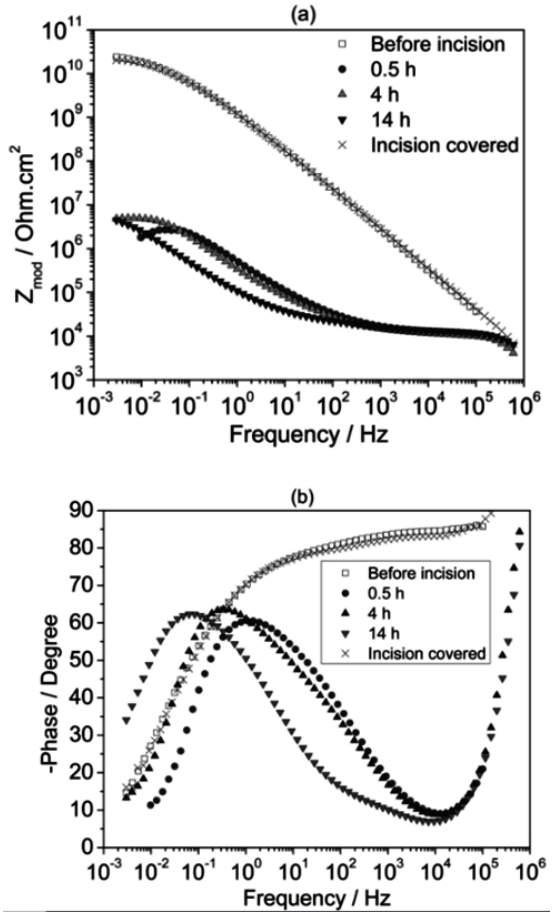

Figure 11. Bode (A) and Phase (B) diagrams for the coating before and after a 5 mm incision

When the coating has a defect, the overall impedance is related with the corrosion of the substrate, with impedance values 4 orders of magnitude lower than those observed in the absence of a defect. This result was confirmed when impedance measurements were taken of coated samples with the incision covered with paraffin. Paraffin completely covered the incision preventing electrolyte penetration in that area. The impedance values of the coating when the defect was covered with paraffin were similar to those observed in the defect-free coating, which indicates that the impedance actually follows the evolution of the coating defects. In addition, these results indicate that the separation of time constants in the impedance diagrams does not necessarily imply loss of adhesion of the coating or the onset of delamination. Therefore, the breakpoint frequency method for calculating the delaminated area from impedance diagrams, in those cases where it is possible to implement it, would be more suitable for calculating the percentage of the defective area than the delaminated area.

5. CONCLUSIONS

The high anticorrosion performance of the epoxy mastic coating is due to its superior barrier property, which is caused by low water solubility and low diffusivity. During the evaluation of the anticorrosion performance of a polymeric coating by EIS, the modulus of the impedance follows most closely the behavior of the charge transfer resistance than the resistance of the coating, which suggests that the behavior of this parameter should preferably be taken into account when looking at the overall anticorrosive coating performance.

The breakpoint frequency method, which is useful when the two time constants are well differentiated and used traditionally for calculating the delaminated area, could be used to estimate the percentage of the defective area rather than the delaminated area in a coated sample.

ACKNOWLEDMENTS

The authors wish to acknowledge the financial contribution of the “Estrategia de Sostenibilidad 2013-2014 de la Universidad de Antioquia”.

REFERENCES

[1] Haruyama, S., Asari, M. and Tsuru, T., Corrosion Protection by Organic Coatings. in Electrochemical Society (ECS) Proceedings. 1987. Pennington: The Electrochemical Society.

[2] Amirudin, A. and Thierry, D., Application of electrochemical impedance spectroscopy to study the degradation of polymer-coated metals. Progress in Organic Coatings, 26(1), pp. 1-28, 1995.

[3] Piratoba, U., Olaya, J.J. and Mariño, A., Impedancia Electroquímica - Interpretación de diagramas típicos con circuitos equivalentes. Dyna, 77(164), pp. 69-75, 2010.

[4] Popov, B.N., Alwohaibi, M.A. and White, R.E., Using Electrochemical Impedance Spectroscopy as a Tool for Organic Coating Solute Saturation Monitoring. Journal of Electrochemical Society, 140(4), pp. 947-951, 1993.

[5] Stern, M. and Geary, A.L., Electrochemical Polarization. Journal of Electrochemical Society, 104, pp. 56, 1957.

[6] Kending, M., Mansfeld, F. and Tsai, S., Determination of the long term corrosión behavior of coated steel with A.C. Impedance measuremends. Corrosion Science, 23, pp. 317-329, 1983.

[7] Scully, J.R., Electrochemical Impedance of Organic-Coated Steel: Correlation of Impedance Parameters with Long’Term Coating Deterioration. Journal Electrochemical Society, 136, pp. 979-990, 1989.

[8] Hirayama, R. and Haruyama, S., Electrochemical impedance for degraded coated steel having pores. Corrosion, 47, pp. 952-958, 1991.

[9] Deflorian, F. et al., Organic coating capacitance measurement by EIS: ideal and actual trends. Electrochimica Acta, 44, pp. 4243–4249, 1999.

[10] Singh, S.K. et al., Electrochemical impedance study of thermally sprayable polyethylene coatings. Corrosion Science, 51(3), pp. 595-601, 2009.

[11] Westing, E.P.M.V., Ferrari, G.M. and Wit, J.H.W.D., The determination of coating performance with impedance measurements - II. water uptake of coatings. Corrosion Science, 36, pp. 957-977, 1994.

[12] Barsoukov, E. and Macdonald, J.R., Impedance Spectroscopy Theory, Experiment, and Applications. 2 ed. 2005: John Wiley and Sons, Inc.

[13] Shreepathi, S. et al., Service life prediction of organic coatings: electrochemical impedance spectroscopy vs actual service life. Journal of Coatings Technology and Research pp. 191-200, 2010.

[14] Miszczyk, A. and Darowicki, K., Multispectral impedance quality testing of coil - coating system using principal component analysis. Progress in Organic Coatings, 69, pp. 330-334, 2010.

[15] Hsu, C.H. and Mansfeld, F., Concerning the Conversion of the Constant Phase Element Parameter Y0 into a Capacitance. Corrosion, 57, pp. 747-748, 2001.

[16] Bierwagen, G. et al., EIS studies of coated metals in accelerated exposure. Progress in Organic Coatings, 46(2), pp. 149-158, 2003.

[17] Parka, J.H. et al., The improvement of anticorrosion properties of zinc-rich organic coating by incorporating surface-modified zinc particle. Progress in Organic Coatings, 74(1), pp. 25-35, 2012.

[18] Hu, J.M., Zhang, J.Q. and Cao, C.N., Determination of water uptake and diffusion of Cl- ion in epoxy primer on aluminum alloys in NaCl solution by electrochemical impedance spectroscopy. Progress in Organic Coatings, 46, pp. 273-279, 2003.

[19] Deflorian, F. and Rossi, S., An EIS study of ion diffusion through organic coatings. Electrochimica Acta, 51, pp. 1736-1744, 2006.

[20] Brasher, D.M. and Kingsbury, A.H., Electrical measurements in the study of immersed paint coatings on metal. I. Comparison between capacitance and gravimetric methods of estimating water-uptake. Journal of Applied Chemistry, 4, pp. 62-72, 1954.

[21] Rammelt, U. and Reinhard, G., Application of electrochemical impedance spectroscopy (EIS) for characterizing the corrosion-protective performance of organic coatings on metals. Progress in Organic Coatings, 21, pp. 205-226, 1992.

[22] Castela, A.S. and Simoes, A.M., An impedance model for the estimation of water absorption in organic coatings. Part II: A complex equation of mixture. Corrosion Science, 45, pp. 1647-1660, 2006.

[23] Westing, E.P.M.V., Ferrari, G.M., and Wit, J.H.W.D., The determination of coating performance with impedance measurements. Electrochemical Acta, 7, pp. 899-910, 1994.

[24] Socrates, G., Infrared and Raman Characteristic Group Frequencies: Tables and Charts, ed. L. John Wiley and Sons. 2001, London.

[25] Goresy, A.E. et al., Natural shock-induced dense polymorph of rutile with α-PbO2 structure in the suevite from the Ries crater in Germany. Earth and Planetary Science Letters, 192, pp. 485-495, 2001.

[26] Vašková, H. and Křesálek, V., Quasi real-time monitoring of epoxy resin crosslinking via Raman microscopy. International Journal of Mathematical Models and Methods in Applied Sciences, 5, pp. 1197-1204, 2011.

[27] Kendig, M.W. and Henry Leidheiser, J., The Electrical Properties of Protective Polymer Coatings as Related to Corrosion of the Substrate. Journal of Electrochemical Society, 123(7), pp. 982-989, 1976.

[28] Pistorius, P.C., Electrochemical testing of "intact" organic coatings. in 14th International Corrosion Congress. 1999. Cape Town.

[29] Gray, L.G.S. and Appleman, B.R., EIS: Electrochemical Impedance Spectroscopy A Tool To Predict Remaining Coating Life? Journal of Protective Coatings & Linings, 30, pp. 66-74, 2003.

[30] Legghe, E. et al., Correlation between water diffusion and adhesion loss: Study of an epoxy primer on steel. Progress in Organic Coatings, 66(3), pp. 276-280, 2009.

[31] Krzak, M. et al., Water diffusion in polymer coatings containing water-trapping particles. Part 2. Experimental verification of the mathematical model. Progress in Organic Coatings, pp. 207-214, 2012.

[32] Thomas, N.L., The barrier properties of paint coatings. Progress in Organic Coatings, 19, pp. 101-121, 1991.